Original Article

Institution of MECHANICAL ENGINEERS
Journal of AEROSPACE ENGINEERING

Proc IMechE Part G:
J Aerospace Engineering
0(0) 1–12

DOI: 10.1177/0954410018795815
journals.sagepub.com/home/pig
SAGE

Conceptual design methodology of a box wing aircraft: A novel commercial airliner

Pavlos Kaparos, Charalampos Papadopoulos and Kyros Yakinthos

Abstract

In this work, the development of a conceptual design methodology of an innovative aircraft configuration, known as box wing, is presented. A box wing aircraft is based on a continuous-surface nonplanar wing formation with no wing-tips. The A320 medium range conventional cantilever wing aircraft is used as both the reference aircraft and the main competitor of the box wing aircraft. Based on the A320 characteristics and dimensions, a complete aerodynamic analysis of the box wing configuration is made by means of layout design and computational fluid dynamics studies, highlighting the aerodynamic and operating advantages of the box wing configuration compared to the A320 aircraft. The aspect ratio and the Oswald factor of a box wing aircraft differ significantly from the corresponding ones of A320 and provide increased aerodynamic performance. The increased aerodynamic performance leads by consequence, to lower fuel consumption, thus allowing longer range for the same payload or greater payload for the same range, contributing to the efforts for greener environment. In this work, the design methodology begins by estimating the critical initial design parameters, such as aspect ratio, dihedral angle, sweep angle, and taper ratio, which are continuously refined via an iterative process based on a conceptual design study. Various flying scenarios are studied using computational fluid dynamics and analytical calculations, in order to compare the performance of the box wing and the conventional A320, having always the same mission and payload conditions. The conceptual results show that the novel box wing configuration has considerable aerodynamic performance advantages compared to the conventional A320 aircraft.

Keywords

Box wing, layout design, Oswald factor, novel aircraft design, conceptual design

Date received: 12 January 2018; accepted: 13 July 2018

Introduction

The Advisory Council for Aeronautics Research in Europe (ACARE) has set strict goals[1] regarding the NO_x and CO_2 emissions, which are produced by the operating civil aircrafts. These goals are based on the increasing rate of the air transportation that nowadays contributes about 2% to the global man-made emissions[2] as shown in Figure 1.

In order to achieve these environmental targets, a reduction in fuel consumption, which proportionally leads to a pollutant emissions reduction, is obligatory. Fuel saving of an aircraft and, consequently, reduction of the pollutant emissions can be mainly achieved by minimizing the total aerodynamic drag. This could be accomplished through better technologies, lighter materials, alternative fuels, or electrification of the propulsion. However, a different aircraft design approach can also lead to a more efficient aircraft than a conventional one. Such a design is the joined wing configuration. At the beginning of the previous century, it was suggested that the lifting system with the minimum induced drag is a proper box-like wing as shown in Figure 2, also named "Best Wing System", a closed wing surface with no wingtips whatsoever.[3] Prandtl's box wing design connects the tips of two offset horizontal wings with vertical wings shaped to provide a linear distribution of side forces.

While reviewing the literature, it became obvious that there is a relative scarcity of information with regards to conceptual design of box wing aircrafts. Kroo[4] and Wolkovitch[5] set the fundamental elements for the box wing research. Schiktanz and Scholz[6] set up various definitions of terms that are considered as

Laboratory of Fluid Mechanics and Turbomachinery, Department of Mechanical Engineering, Aristotle University of Thessaloniki, Thessaloniki, Greece

Corresponding author:
Kyros Yakinthos, Laboratory of Fluid Mechanics and Turbomachinery, Department of Mechanical Engineering, Aristotle University of Thessaloniki, Thessaloniki 54124, Greece.
Email: kyak@auth.gr

fundamental and gave a general approach on the design and aerodynamic analysis. Jemitola and Fielding[7] focused more on the structural challenges of a box wing aircraft rather than the aerodynamic characteristics and Frediani[8] also focuses on the interior design and structural requirements of a box wing aircraft. Thus, given the situation, the authors of the present work tried to fill this gap in the literature, by formatting an analytical methodology of the box wing aerodynamic conceptual design based on previews experience in conventional aircraft design.[9]

As mentioned by Kroo,[4] a box-like wing aircraft has 30% less induced drag than a conventional aircraft. Additionally, this novel configuration is lighter than the conventional one as referred by Wolkovitch.[5] Based on these advantages, a conceptual design procedure of a commercial mid-range box wing aircraft and a comparison with a conventional one are carried out in the current work. The reference aircraft that is used in this paper as the baseline aircraft is the Airbus A320 commercial airliner. It is a typical medium range conventional cantilever wing aircraft, widely used all over Europe and the rest of the world. This work emphasized on the aerodynamic design methodology of a box wing aircraft configuration utilizing both computational fluid dynamics (CFD) and in-house developed and validated design tools that are based on aircraft design textbooks.[10,11]

Mission requirements

The aim of the study was to design a 180 passengers box wing aircraft with similar characteristics as the reference aircraft (A320). As a result, the design range was set to be 4000 km at a speed of 0.78 M, a cruise altitude of 37,000 ft, and a maximum take-off distance of 2000 m. All the aforementioned mission requirements are presented in Table 1.

As seen in Figure 3, the aircraft follows a typical mission profile. After the warm-up period, the aircraft takes off and climbs up to 35,000 ft. After reaching the targeted area, the aircraft enters a period of 20 min[12] of loitering before it finally lands.

Conceptual design

During the conceptual design phase, a first configuration layout is developed. Figure 4 shows the

Table 1. Box wing mission requirements.

Payload weight	16.8 tons (180 passengers)
Range	4000 km
Cruise speed	0.78 M
Cruise altitude	35,000–40,000 ft
Take-off distance	2000 m

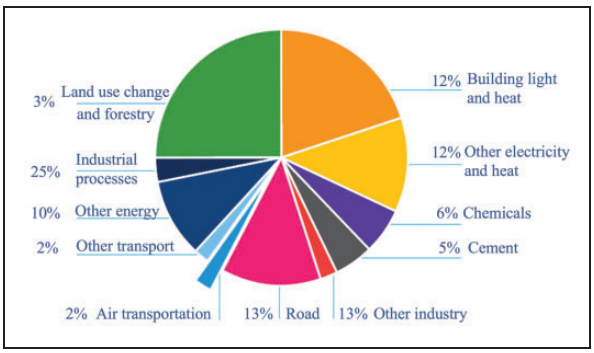

Figure 1. Global man-made emissions.[2]

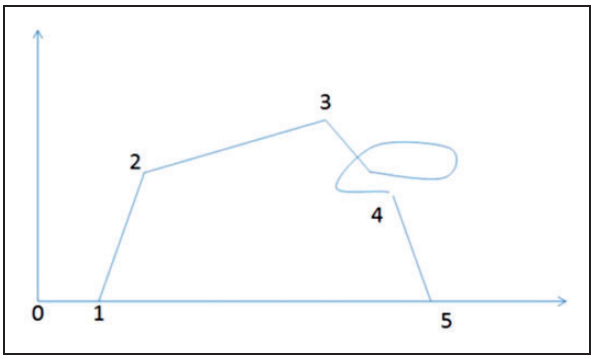

Figure 3. Mission profile of the box wing aircraft.

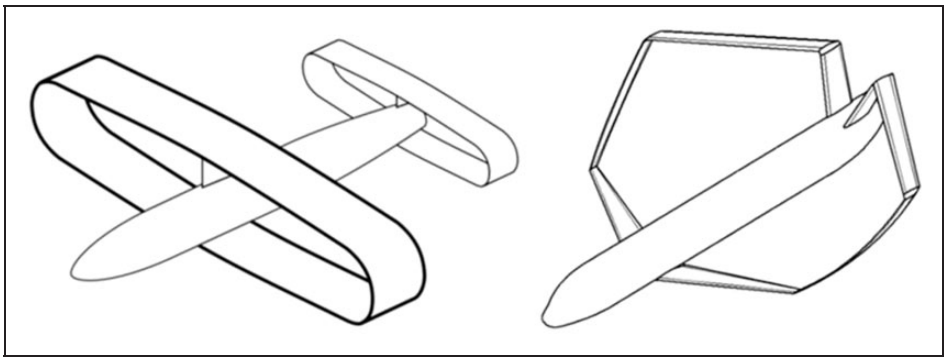

Figure 2. An annular closed wing design and the author's concept.

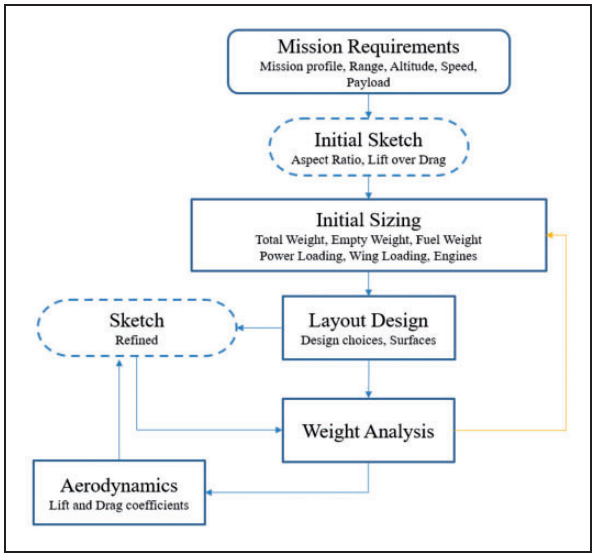

Figure 4. Conceptual design roadmap.

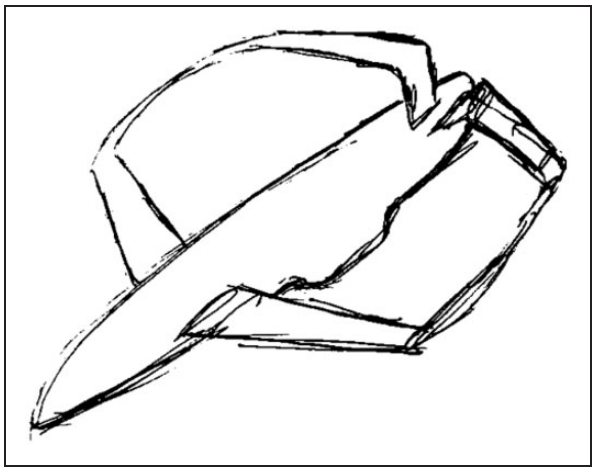

Figure 5. First rough sketch of the box wing configuration.

breakdown of the conceptual design. First estimates regarding geometry, weight, aerodynamics, and performance are calculated, according to the mission requirements. In the present study, an excel-based spreadsheet tool, relying on aircraft design textbooks,[10,11] was developed. However, in order to take the novel design of the box wing configuration into account, numerous modifications, including the AR and the Oswald factor, have been performed. Furthermore, it is worth mentioning that during this phase of the design procedure no optimization study has been carried out.

Initial sizing

Once the mission requirements were established and the first rough sketch of aircraft, as a ''back of the napkin sketch'' was developed (Figure 5), the initial sizing began. Based on the empirical and statistical data, as well as analytical equations, a series of characteristic parameters were estimated. Such parameters

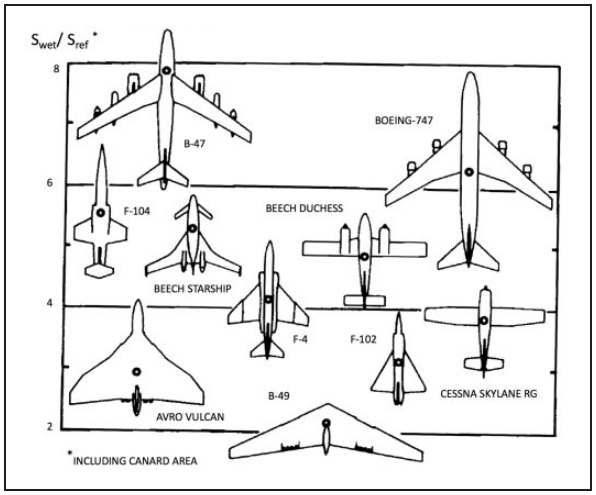

Figure 6. Wetted area ratios, trends for different types of aircraft.[11]

include the total weight of the aircraft (W_0), the thrust-to-weight ratio (T/W), and the weight-to-surface ratio (W/S).

Starting from historical trends (Figure 6) and applying an iterative procedure, the total weight of the aircraft was calculated. The weight fractions for each mission segment were calculated, as shown in Figure 3. Furthermore, the thrust-to-weight ratios were estimated for different scenarios and the worst-case scenario was chosen in order assure that the aircraft will be able to safely accomplish the flight mission.[11,12] With the T/W ratio and the total weight being known, the thrust required was extrapolated in a way that ensures a proper operationality of the aircraft. According to the calculated thrust, appropriate engines were chosen. The final crucial variable is the reference area (S_{ref}). Again, a series of W/S ratios is computed. The least favoring scenario is picked in order to ensure the best operational capabilities of the aircraft.

For the completion of these early calculations, the values of the Oswald efficiency factor (e) and the aspect ratio (AR) are needed. These two parameters differ significantly from conventional aircrafts, due to the special aerodynamic shape of the box wing aircraft. The great advantage of this novel configuration, as is highlighted in the literature, is the low induced drag.[4] Both these parameters are taken into account in the calculation of the induced drag (equation (1)). In the current work, the authors designed the aircraft so that the front and aft wing of the box wing configuration have equal span (b). The total reference area of the aircraft is S, and the reference area of each wing is S_1 and S_2, respectively. Based on these areas, the total aspect ratio (AR_{tot}) is calculated by equation (2). If this approach is applied in the one wing, the AR is twice the AR_{tot} as shown in equation (3)

$$C_{Di} = \frac{C_L^2}{\pi \cdot AR \cdot e} \tag{1}$$

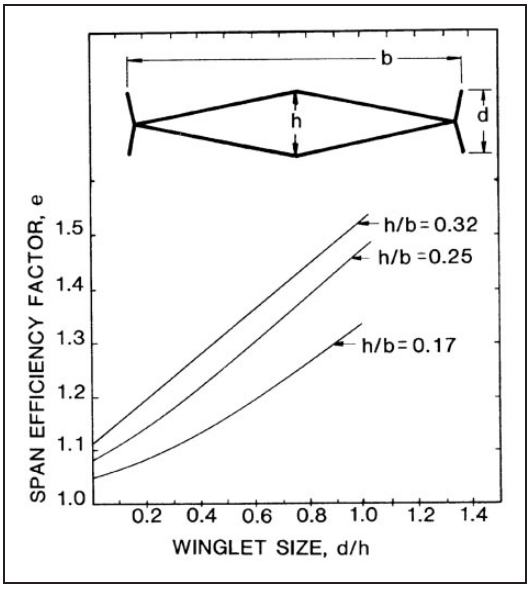

Figure 7. Span efficiency factor for joined wings.[5]

$$AR_{tot} = \frac{b^2}{S} = \frac{b^2}{S_1 + S_2}, \quad \text{where } S_1 = S_2 = \frac{S}{2} \tag{2}$$

$$AR_1 = \frac{b^2}{S_1} = \frac{b^2}{\frac{S}{2}} = 2 \cdot \frac{b^2}{S} = 2 \cdot AR_{tot} \tag{3}$$

In the design phase of this work, the value of the AR was chosen to be equal to 15.5. This will further reduce the induced drag of each wing. Schiktanz and Scholz[6] also followed this design philosophy.

The Oswald efficiency factor is a factor that represents the change in drag with lift of a three-dimensional structure as opposed to an ideal one, with the same aspect ratio and with an elliptical lift distribution. Wolkovitch,[5] based on theoretical analyses of Letcher,[13] generated a theoretical approach for the span efficiency factor for joined wings (Figure 7).

The approach though, consists of some assumptions and therefore a correction has to be made. Wolkovitch and Bettes[14] experimentally proposed a correcting equation (4) regarding the calculation of the span efficiency factor (Oswald factor). More specifically, in this experimental study,[14] a joined-wing and a conventional wing aircraft with the same fuselage were tested. In their work, Wolkovitch and Bettes[14] in order to analytically calculate the Oswald factor used the method proposed by Letcher.[13] This method proved that the joined-wing aircraft has a theoretical span efficiency factor 4% larger than the conventional aircraft. However, the experiments[14] indicated that this difference was, in reality, 9%. Eventually, according to these results, Wolkovitch and Bettes[14] constructed a correction formula between the actual and the theoretical Oswald factor, as described by equation (4). The values 29° and 20° in the denominator of equation (4) represent the front and rear sweep angles respectively of the reference joined-wing aircraft, which Wolkovitch and Bettes[14] utilized in their experimental work.[14]

Table 2. Oswald factor using different calculation methods.

Calculation method	Oswald factor (e)
Wolkovitch[5]	1.43
Nita and Scholz[15]	1.44
Kroo[4]	1.46

$$\frac{e_{actual}}{e_{theoretical}} = 1 + \frac{0.04(\tan\Lambda_F + \tan\Lambda_R)}{(\tan 29^\circ + \tan 20^\circ)} \tag{4}$$

From equation (4), it becomes evident that this correction formula takes into account the sweep angles of the front and rear wing (Λ_F and Λ_R). Thus, in the current work, the calculation of the span efficiency factor does take into account the high sweep angles of the proposed box wing aircraft.

However, the Wolkovitch's[5] wing configuration does not integrate the winglets to create a more rectangular wing geometry. Consequently, in order to consider the effect of the winglets, which connect the front and rear wing of the proposed box wing configuration, some modifications were necessary. The Oswald factor was estimated twice using the proposed by the literature methods[4,15] that takes into account the vertical winglets shape. Table 2 shows the calculated Oswald factor (e) for the total three different methods. Based on these results, the authors make the assumption that even though Wolkovitch's wing configuration does not integrate the winglet to create a more rectangular wing geometry, the difference in the span efficiency factor would be negligible and the Wolkovitch's[5] correction equation has the potential to correctly calculate the span efficiency factor of a box wing configuration.

The authors select the minimum value of the three calculated Oswald factors in order to have a conservative approach regarding the aerodynamic performance calculations of the proposed box wing configuration.

Layout design

As it has been stated already, the reference conventional aircraft is the A320-200. All the geometrical characteristics regarding the A320-200 are presented in Table 3.[16] In the current study, all the basic geometric parameters are not only very close to the reference (A320-200) ones but also in accordance with the calculations according to the design methodology of Raymer.[11] The reference wing area, the length of the fuselage, and the diameter of the aircraft deviate only a little from the original values.

Table 3. Geometrical characteristics of the reference aircraft[16] and the proposed box wing configuration.

Parameter	A320-200	Proposed box wing	Difference
Wingspan, b	33.7 m	30 m	−10.9%
Fuselage length, $l_{fuselage}$	40.8 m	39.4 m	−3.4%
Fuselage diameter, $\varnothing_{fuselage}$	4.2 m	4 m	−4.7%
Sweep front wing, Λ_{front}	25°	29°	16%
Sweep aft wing, Λ_{aft}	–	−35°	–
Taper ratio front wing, λ_{front}	0.24°	0.25°	4.1%
Taper ratio aft wing, λ_{aft}	–	0.8°	–
Dihedral front wing, Γ_{front}	5.1°	6°	17.6%
Dihedral aft wing, Γ_{aft}	–	−2	–
Wing aspect ratio, AR_{wing}	9.39	15.5	65%
Oswald factor, e	0.9	1.43	58.9%
Surface area, S_{ref}	121 m^2	105 m^2	−13.2%
Maximum take-off weight, MTOW	77,330 kg	69,800 kg	9.7%

The interior layout was designed according to Torenbeek,[17] so that it resembles a classic medium range aircraft. It is important to note that a designer should consider pilot's view angles and the angle of the tail of the aircraft, so that the aircraft fuselage does not touch the ground when taking off.

Since the cruise Mach number of the two aircrafts is equal, a good starting point for the sweep angles of the box wing aircraft is the sweep angle of the reference aircraft. In order to simplify the design, both wings of the proposed box wing are initially set to the same sweep angle of ±25°. Schiktanz and Scholz[6] claim that an increase in the sweep angle is necessary in order to meet the transonic requirements. Furthermore, functional and spatial challenges led to an even increased sweep angle for the aft wing. The position of the forward wing is limited by the passenger door, as a 1 m clearance should be kept.[6,18] The aft wing sweep is chosen in such a manner that the sweep of the vertical winglets would not become too high. Finally, the complete wing configuration has to comply with the center of gravity (CG) of the whole aircraft.[6,18] Therefore, the final sweep angles are set to +29°/−35°. The taper ratio of the A320 wings is 0.24. Almost the same value (0.25) is chosen for the front wing's taper ratio, following the literature-driven average.[6,11] For instance, the Boeing B-737 aircraft has a taper ratio about 0.25.[19] Taking into account the given wing reference area, and to ensure a sufficient root chord length, a tapper ratio of 0.8 is chosen for the aft wing. This decision was influenced by the possible structural issues, the flap integration[18] and the integration of the vertical winglets.

Low wing aircraft, such as the A320, or the front wing of authors' model, suffer from lack of lateral stability.[18] In order to counter this problem, a 6° dihedral for the front wing is applied. Shoulder wing aircraft have an increased lateral stability. Even though an anhedral design would lower the lateral stability, the advantageous 2° anhedral in the aft wing is chosen in order to reduce the vertical distance between the two wings and, consequently, the total weight of the aircraft. As for the tail of the aircraft, the authors ended up with a V-tail design. V-tails are being well known not only for their stability[11] but also for their spin recovery characteristics that are at least as good as these of a conventional tail, as mentioned by Purser and Campbell.[20] Putting their various benefits aside, a V-tail design would support favorably the two separate aft wings.

The airfoils used should not only have good aerodynamic properties, but also discourage the formation of shock waves. Various airfoils were studied and categorized according to these criteria. The authors concluded to the use of NACA 63-415 and GRUMMAN K-2 as the root and tip airfoils, respectively. Frediani[8] also used the GRUMMAN K-2 airfoil due to its good lift-to-drag ratio and high Mach critical number (M_{crit}). M_{crit} served also as a criterion for the NACA 63-415 airfoil. In addition, the root airfoil was selected due to its high thickness ratio (15%). Both airfoils were analyzed using the method proposed by Heinemann et al.[21] In Figure 8, the M_{crit} value of each airfoil is presented showing a very good behavior in the high subsonic region.

All the geometrical characteristics of the authors' proposed model are presented in Figure 9.

Weight analysis

After the initial weight analysis, a more complicated and analytical computation takes place. This analysis helps to define the exact position of the CG of the aircraft. It is of utmost importance that the CG comes after the aerodynamic center (AC) of the wings, which is the point where the total lift $(L_{tot})_{wing}$ is applied. In case of a power loss, the aircraft will immediately adapt a positive incidence and therefore will not lose stability. For a more convenient design, we decided to split the lift in half. Both, the

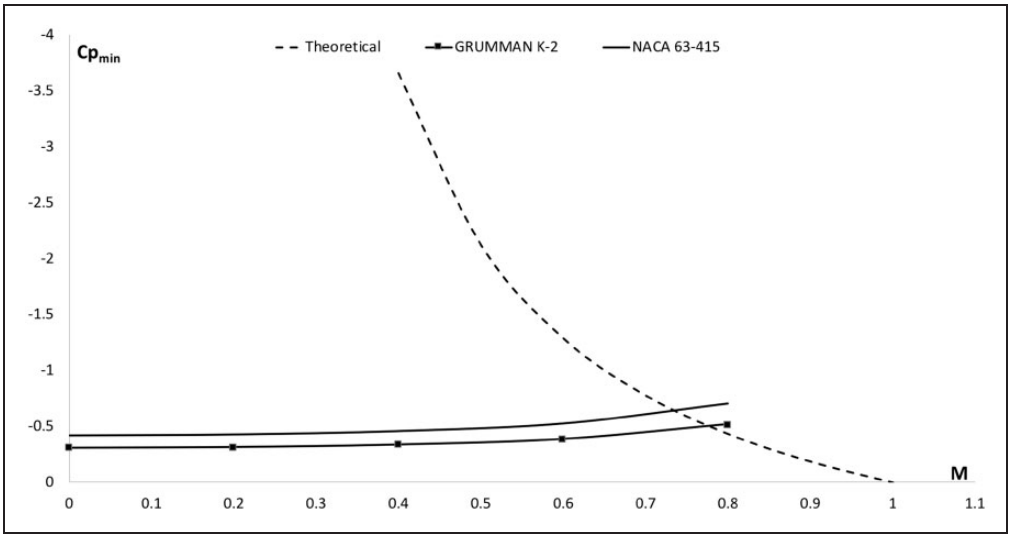

Figure 8. Mach critical characteristics of NACA 63-415 airfoil and GRUMMAN K-2 airfoil.

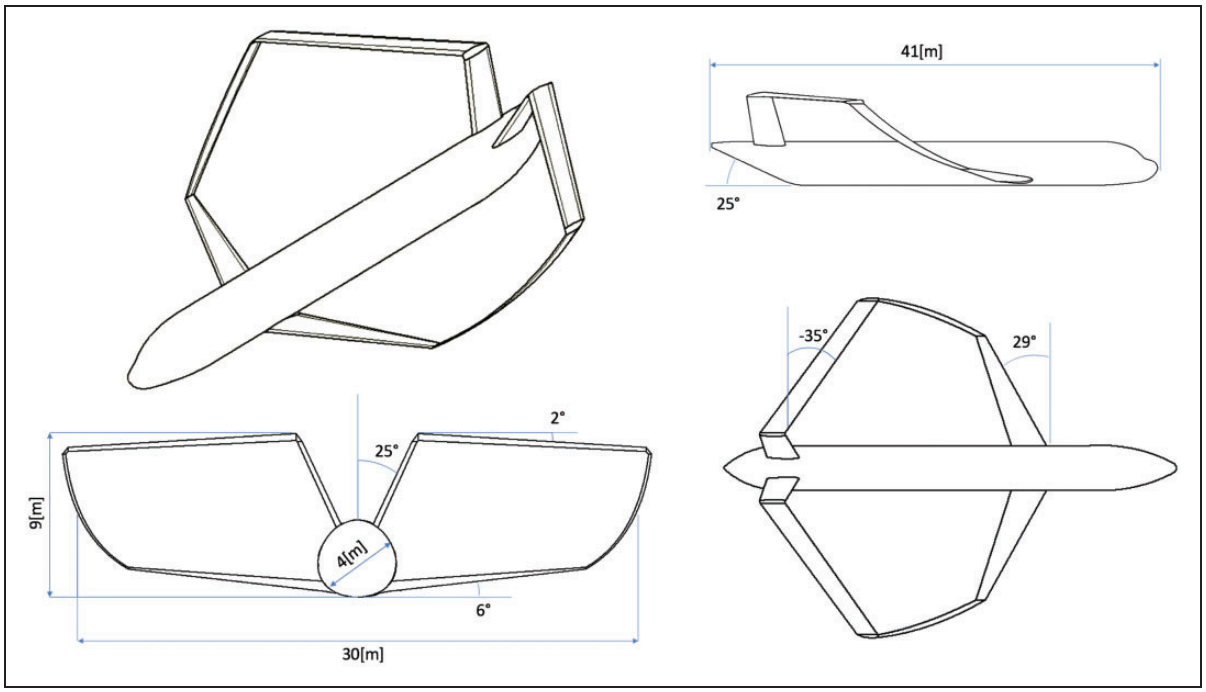

Figure 9. Geometrical characteristics of the author's proposed box wing configuration.

front and the aft wing are designed to generate half of the total lift. Therefore, the total surface was split equally between these two wings, while using the same set of airfoils for both wings. As mentioned before, the total AC of the wings should be in front of the CG. In Figure 10(a), the location of each component's CG and the total box wing's CG are presented. On the other hand, Figure 10(b) depicts the location of the total AC of the wings ($AC_{tot,wing}$) and the total aircraft's AC ($AC_{tot,aircraft}$). $AC_{tot,aircraft}$ is calculated using the CFD results, as the point where the gradient of the total aircraft's moment coefficient $(C_M)_{total}$ due to the aircraft's angle of attack is zero $\left(\frac{dC_M}{da} = 0\right)$.

$AC_{tot,wing}$ is defined as the mean distance between each wing's quarter mean aerodynamic chord (MAC). The CG location is heavily affected by the engines being mounted on the aft wings as shown in Figure 10(a). Furthermore, in this phase of the design procedure, an analytical weight breakdown was carried out and the weight of each aircraft part was calculated as proposed by Schiktanz[6] and Raymer.[11] In Table 4, the weight breakdown and the CG of each part of the aircraft is presented.

As shown in Table 3, the calculated MTOW of the proposed aircraft is about 10% smaller than the reference aircraft. This difference between the MTOW of the proposed box wing and the reference aircraft is

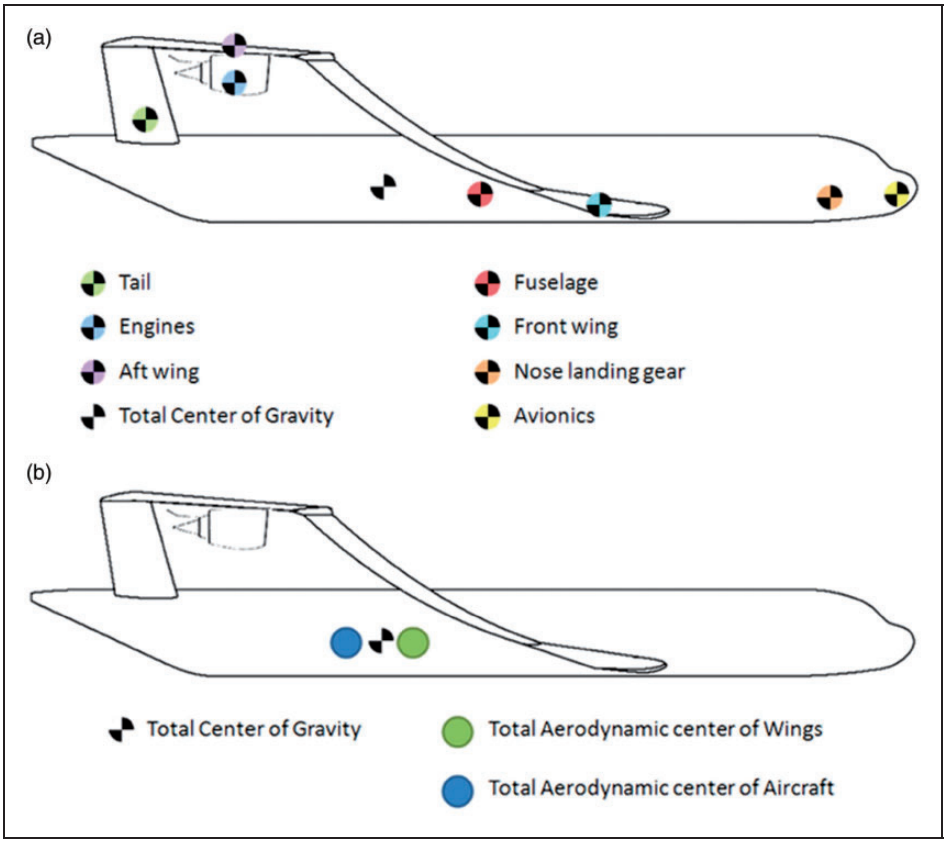

Figure 10. (a) Location of each component's CG and the total box wing's CG, and (b) location of the total AC of the wings and the total aircraft's AC.

Table 4. Aircraft's weight breakdown.

Aircraft part	Weight (kg)	CG position (m)	Aircraft part	Weight (kg)	CG position (m)
Front wing	1914	15.7	Fuel system	836	Distributed[a]
Aft wing	2255	32.6	Flight controls	4632	Distributed[a]
Horizontal tail	316	36.1	Hydraulics	69	20.5
Vertical tail	332	36.1	Avionics	661	1
Fuselage	5989	20.5	Electrical	355	20.5
Engines	8869	32.2	Air condition and anti-ice	7143	20.5
Main landing gear	1571	20.5	Furnishings	3996	20.5
Nose landing gear	299	4.4	Fuel	13,927	Distributed[a]
		Total aircraft weight (kg)		69,848	24.1

CG: center of gravity.
[a]These components are distributed accordingly to the available control surfaces and wing volume.

due to the difference in the wing's total reference area (S_{ref}), which is about 13% smaller for the box wing than the reference aircraft, as shown in Table 3. The wing's weight is calculated by the box wing weight estimation method proposed by Schiktanz[18] where the unconventional configuration of aircraft's wing is taken into account.

Aerodynamic analysis

As mentioned above, in order to calculate the aerodynamic characteristics of the current box wing aircraft, in-house design tools based on design textbooks[10,11] were used. However, based on the unconventional characteristics of the box wing configuration, some modifications on the equations have been performed as presented below. Regarding the definition of the terms in all of the equations, Appendix shows all the additional details.

In order to calculate the drag coefficient of the proposed box wing, a modification is applied to the original equation from Roskam's methodology,[10] which is shown in equation (5). In the modified equation (6), the term C_{D_w} was converted into the forward

and the aft wing terms, $C_{D_{fw}}$, $C_{D_{aw}}$ respectively. Furthermore, in this equation the V-tail can be projected to a conventional tail and studied as such.[10] The total drag of the forward and aft wing is calculated according to the Roskam's methodology[10] and is given by equation 7(a) and (b) respectively, where the wave drag needs to be applied only when the Mach number is greater than 0.7. The drag-due-to-lift in this equation is a function of the lift produced by the wing and is given in equation (8). If the drag-due-to-lift of the front wing should be examined, the coefficient of lift would be computed according to the Roskam's methodology[10] without any modification, as shown in equation (9)

$$C_D = C_{D_w} + C_{D_{fus}} + C_{D_{ht}} + C_{D_{vt}} \tag{5}$$

$$C_D = C_{D_{fw}} + C_{D_{aw}} + C_{D_{fus}} + C_{D_{ht}} + C_{D_{vt}} \tag{6}$$

$$C_{D_{fw}} = C_{D_{0_{fw}}} + C_{D_{L_{fw}}} = \left(C_{D_{0_{fw_{M0.6}}}} + C_{D_{0_{fw_{wave}}}} \cdot \frac{S_{fw}}{S}\right) + C_{D_{L_{fw}}} \tag{7a}$$

$$C_{D_{aw}} = C_{D_{0_{aw}}} + C_{D_{L_{aw}}} = \left(C_{D_{0_{aw_{M0.6}}}} + C_{D_{0_{aw_{wave}}}} \cdot \frac{S_{aw}}{S}\right) + C_{D_{L_{aw}}} \tag{7b}$$

$$C_{D_{L_{fw}}} = \frac{C_L^2}{\pi \cdot AR \cdot e} \tag{8}$$

$$C_{L_{fw}} = C_{La_w}(a + i_{fw} - a_{0_{L_{fw}}}) \tag{9}$$

However, regarding the aft wing, the lift coefficient (C_L) cannot be calculated as a simple wing, because it operates under the downwash effect appearing on the front wing and also, it cannot be studied as a plain horizontal tail. Therefore, a modified formula combining both a wing and a horizontal stabilizer must be used. The lift coefficient of the aft wing is calculated according to the in-house modified equation (10). More specifically, a modification on equation (9) was made in order to combine both the two aft-wing's roles, one as a horizontal tail and another as an aft wing that operated under the downwash effect. Thus, the modification is made with the additional term $(1 - \frac{d\varepsilon}{da_{aw}})$ that integrates the downwash effect.

$$C_{Law} = C_{L_{a_{aw}}}\left[a\left(1 - \frac{\mathrm{d}\varepsilon}{da_{aw}}\right) + i_{aw} - a_{0_{Law}}\right] \tag{10}$$

In order to calculate the lift curve slope of the aircraft, a combination of the lift curve slopes of the two wings (forward and aft) and the projected horizontal tail is needed. Thus, a modification on the original equation (11) of the Roskam's methodology[10] was made in order for the aft wing to be treated as a horizontal tail. For this reason, in the modified equation (12), the term $[C_{L_{a_{aw}}}\eta_{aw}\frac{S_{aw}}{S}(1 - \frac{d\varepsilon}{da_{aw}})]$ was used. In addition, in this equation the terms $\frac{S_{fw}}{S}$ and $\frac{S_{aw}}{S}$ were added in order to have a weighted surface ratio between the forward and aft wing. In the same way, for the calculation of the zero angle of attack of the aircraft, a modified version of Roskam's equation[10] was used. The original equation (13) is modified to equation (14) to treat the aft wing as a horizontal empennage. Thus, the term $[C_{L_{a_{aw}}}\eta_{aw}\frac{S_{aw}}{S}(i_{aw} - \varepsilon_{aw})]$ is added to equation (14) to take into account the downwash within the aft wing operates. Additionally, similar to equation (12) a weighted surface ratio between the forward and aft wing is derived, by adding the $\frac{S_{fw}}{S}$ and $\frac{S_{aw}}{S}$ terms for the forward and aft wing respectively

$$C_{La} = C_{L_{awf}} + C_{L_{a_{ht}}} \cdot \eta_{ht}\frac{S_{ht}}{S}\left(1 - \frac{d\varepsilon}{da_{ht}}\right) \tag{11}$$

$$C_{La} = C_{L_{awf}}\frac{S_{fw}}{S} + C_{L_{a_{aw}}} \cdot \eta_{aw}\frac{S_{aw}}{S}\left(1 - \frac{d\varepsilon}{da_{aw}}\right) + C_{L_{a_{ht}}}\eta_{ht}\frac{S_{ht}}{S}\left(1 - \frac{d\varepsilon}{da_{ht}}\right) \tag{12}$$

$$C_{L0} = C_{L_{0wf}} + C_{L_{a_{ht}}}\eta_{ht}\frac{S_{ht}}{S}(i_{ht} - \varepsilon_h) \tag{13}$$

$$C_{L0} = C_{L_{0wf}}\frac{S_{fw}}{S} + C_{L_{a_{aw}}}\eta_{aw}\frac{S_{aw}}{S}(i_{aw} - \varepsilon_{aw}) + C_{L_{a_{ht}}}\eta_{ht}\frac{S_{ht}}{S}(i_{ht} - \varepsilon_h) \tag{14}$$

Finally, in order to calibrate and verify the modified in-house design tool, a CFD analysis was carried out. The commercial code Ansys CFX (ANSYS@ Scientific Research, Release 16.1) was used. The computational grid, shown in Figure 11, consisted of approximately 8,800,000 computational nodes. Eighteen inflation layers were generated in order to have for the first layer a distance from the wall equal to 1.2×10^{-5} m, ensuring that the boundary layer development is accurately modeled. The Reynolds-averaged Navier–Stokes (RANS) equations were solved being coupled with the Spalart–Allmaras[22] turbulence model, which has been proven to be capable of providing accurate results for external flows governed by appearing favorable or adverse pressure gradients. In order to calibrate the conceptual design tool, two in-flight conditions were selected. One at sea-level altitude ($M = 0.25$), and one at cruise altitude of 35,000 ft (cruise speed $M = 0.78$), where compressibility effects are present. Regarding the turbulence parameters, the eddy viscosity ratio and the turbulence intensity freestream values were set to 0.2 and 1% respectively, which are considered as typical flight conditions.[23]

Results

The aim of the current work was to build a spreadsheet-based design tool that would accurately estimate the aerodynamic properties of a box wing medium range

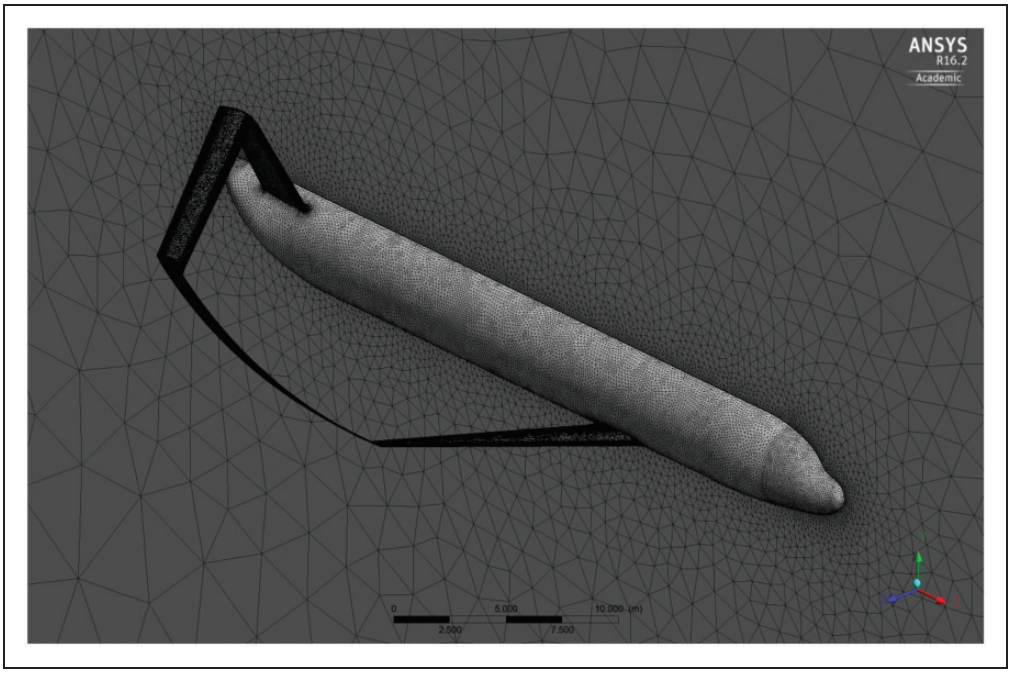

Figure 11. Computational grid on the surface of the proposed box wing configuration.

Table 5. Proposed box wing specifications.

Parameter	A320-200	Proposed box wing	Difference
Wingspan, b	33.7 m	30	−10.9%
Fuselage length, $l_{fuselage}$	40.8 m	39.4	−3.4%
Fuselage diameter, $\varnothing_{fuselage}$	4.2 m	4	−4.7%
Sweep front wing, Λ_{front}	25°	29°	16%
Sweep aft wing, Λ_{aft}	–	−35°	–
Taper ratio front wing, λ_{front}	0.24°	0.25°	4.1%
Taper ratio aft wing, λ_{aft}	–	0.8°	–
Dihedral front wing, Γ_{front}	5.1°	6°	17.6%
Dihedral aft wing, Γ_{aft}	–	−2°	–
Wing aspect ratio, AR_{wing}	9.39	15.5	65%
Oswald factor, e	0.9	1.43	58.9%
Surface area, S_{ref}	121 m^2	105 m^2	−15.2%
Fuel weight, W_{fuel}	13,977 kg	13,927 kg	−0.35%
Cruise speed (Mach), M_{cruise}	0.78	0.78	–
Maximum take-off weight, MTOW	77,330 kg	69,800 kg	−9.7%

aircraft. Based on the design methodology for conventional cantilever aircraft, an in-house tool was developed. In order to verify the results of this tool, a comparison between the CFD and the in-house design tool results was carried-out. In Table 5, the basic specifications of the proposed box wing configuration and the reference aircraft A320-200 are presented.

In Figure 12, the CFD results at cruise conditions are presented. More specifically, the Mach number distribution on the wings and the fuselage is shown. It is clear that in the cruise conditions ($M = 0.78$), compressibility effects are present. These results justify the drag coefficient increase, which is observed in Figure 13. The existence of the compressibility effect in this flight condition leads to the activation of the wave drag term in equation (6), which is used in the in-house design tool. Figure 13 shows the comparison between the CFD and in-house tool results regarding the drag coefficient of the proposed box wing aircraft. The results correspond to both cruise speed ($M = 0.78$) and low-speed ($M = 0.25$) conditions.

A sufficient close behavior, both trendwise and numerically, is observed. The minimum value of the drag coefficient is close to an angle of attack of −2°. These results show that the in-house design tool is more accurate in the low-speed segment of the flight, where the compressibility effects are not present. However, on the cruise segment ($M = 0.78$), it is

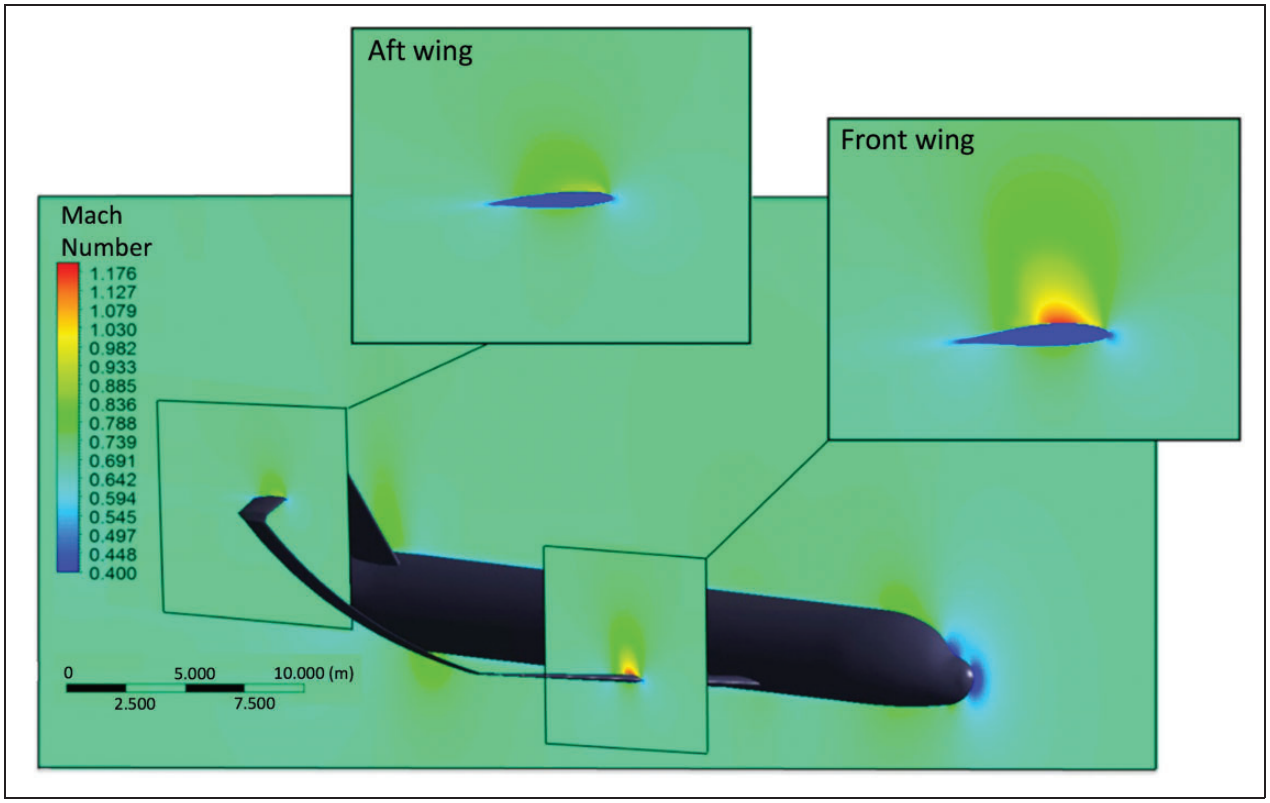

Figure 12. Mach number distribution on wings and fuselage at cruise conditions.

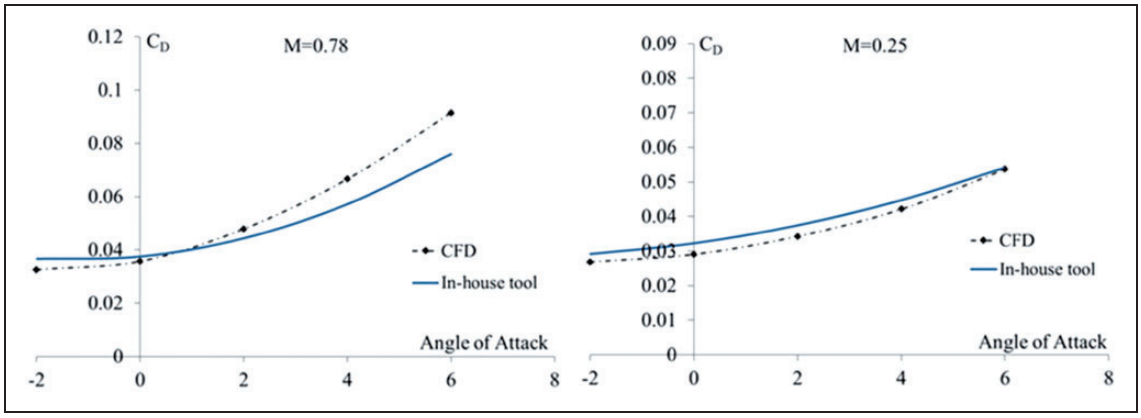

Figure 13. Drag coefficient comparison between CFD and the in-house tool for $M = 0.78$ (left) and $M = 0.25$ (right). CFD: computational fluid dynamics.

worth mentioning that for level flight, the in-house tool results presents a very good agreement with the CFD computations.

After the comparison and verification of the in-house design tool, a comparative study between the proposed box wing configuration and the reference aircraft A320-200 was carried out. Based on the same requirements and the same geometrical restrictions, the comparison is focused on the drag coefficient of the aircraft which is the crucial factor for the fuel consumption reduction. In Table 6, the drag breakdown of the two aircrafts in cruise conditions is presented. The results of the drag breakdown show that there is a significant reduction of about 12.5% of the induced drag (C_{Di}) for the proposed box wing configuration. However, there is a slight increment of about 5.7% in the parasite drag.

Finally, a study on the potential flight range, while using the same thrust specific fuel consumption (TSFC) as the reference aircraft, was performed. Based on the drag coefficient results, available fuel weight (13.927 kg), and reference area of the aircraft (S_{ref}), the calculated range of the proposed box wing aircraft is 5500 km. According to the literature,[16] the reference aircraft has a range up to 4000 km, proving the box wing configuration to be more efficient. As mentioned in the Table 1, all the initial design requirements are the same for both the reference aircraft and

Table 6. Drag breakdown for the reference A320-200[16] aircraft and the proposed box wing configuration at cruise flight conditions.

Aircraft type	C_{D0} (parasite drag)	Difference	C_{Di} (induced drag)	Difference
Reference A320-200	0.021	5.7%	0.018	−12.5%
Proposed box wing	0.022		0.016	

the proposed box wing. Thus, the payload and the passenger number are the same for both aircrafts. Finally, the MTOW of the proposed box wing aircraft is about 10% smaller than that of the reference aircraft, something that was discussed in the ''Weight analysis'' section.

Conclusions

In the current work, a conceptual design methodology for an unconventional box wing aircraft configuration, using both CFD and modified in-house design tools has been presented. The basic aim of this study was the validation and calibration of the modified in-house design tool via the CFD results for the unconventional box wing aircraft. The reference aircraft, which was used as a baseline design point, is the Airbus A320 commercial airliner. This aircraft is a medium range conventional cantilever wing aircraft, widely used all over the world. Based on this reference aircraft, all the requirements were set up in order to design the novel box wing concept. The second aim of this work was the comparison between the reference A320 aircraft and the new proposed box wing configuration. It must be noticed that in the conceptual design phase, no optimization studies were carried out. Therefore, there is room for further studies regarding layout optimization. The results of the computations showed that the configuration used in this paper offers the potential for improvement.

The developed in-house design tool showed a noticeable capability to predict sufficiently well the aircraft aerodynamic characteristics. Furthermore, the results showed that the proposed box wing aircraft has a lower drag coefficient and, more specifically, lower induced drag coefficient in cruise conditions than the reference aircraft. These results are in accordance with previous research,[16,24] which claimed the reduction of the induced drag (C_{Di}) as an advantage of the box wing configurations.

Declaration of Conflicting Interests

The author(s) declared no potential conflicts of interest with respect to the research, authorship, and/or publication of this article.

Funding

The author(s) received no financial support for the research, authorship, and/or publication of this article.

ORCID iD

Pavlos Kaparos http://orcid.org/0000-0002-2637-8808

References

1. European Commission. Flightpath 2050: Europe's vision for aviation. Report of the High Level Group on Aviation Research, Publications Office of the European Union. Epub ahead of print 2011.
2. Advisory Council for Aviation Research and Innovation in Europe. Strategic Research & Innovation Agenda.
3. Prandtl L. *Induced drag of multiplanes*. National Advisory Committee for Aeronautics, 1924.
4. Kroo I. Nonplanar wing concepts for increased aircraft efficiency. *VKI lecture series on innovative configurations and advanced concepts for future civil aircraft*, 2005, pp.1–29.
5. Wolkovitch J. The joined wing: An overview. In: *23rd aerospace science meeting*, Reno, Nevada, 14–17 January 1985; 1–26.
6. Schiktanz D and Scholz D. Box wing fundamentals – An aircraft design perspective. In: *DGLR Dtsch Luft-und Raumfahrtkongress*, Bonn, Germany, 2011, pp.601–615.
7. Jemitola PO and Fielding JP. Box wing aircraft conceptual design. In: *28th international congress of the aeronautical sciences*, Brisbane, Australia, 2012, pp.1–10.
8. Frediani A. The Prandtl wing. *VKI lecture series on innivative configurations and advanced concepts for future civil aircraft*, 2005, pp.1–23.
9. Panagiotou P, Kaparos P, Salpingidou C, et al. Aerodynamic design of a MALE UAV. *Aerosp Sci Technol* 2016; 1: 1–12.
10. Roskam J. *Airplane design*. Lawrence, KS: DARcorporation, 2004.
11. Raymer DP. *Aircraft design: A conceptual approach*. 5th ed. Reston, VA: American Institute of Aeronautics and Astronautics, 2012.
12. Anderson JD Jr. *Aircraft performance and design*. New York: WCB/McGraw-Hill, 1999.
13. Letcher JS. V-wings and diamond ring – Wings of minimum induced drag. *J Aircraft* 1972; 9: 605–607.
14. Wolkovitch J and Bettes WH. Low-speed wind tunnel test on joined wing and monoplane configurations, Vol. I: Analysis of results, Vol. II: Test data. ACA Report 82-2, 1984, p. 117.
15. Nita M and Scholz D. Estimating the Oswald factor from basic aircraft geometrical parameters. In: *Dtsch Luft- und Raumfahrtkongress*, Berlin, Germany, 10–12 September 2012, pp.1–19.
16. Zohlandt CN. Conceptual design of high subsonic Prandtl planes. TU Delft, https://repository.tudelft.nl/islandora/object/uuid:e1f01743-e2eb-4d8b-8b2c-131f50f41a2c?collection=education (2016, accessed 28 August 2017).

17. Torenbeek E. *Advanced aircraft design: Conceptual design, analysis and optimization of subsonic civil aircraft*. New York: Wiley, 2013.
18. Schiktanz D. *Conceptual design of a medium range box wing aircraft*. Thesis, Hamburg University of Applied Sciences, Germany, 2011.
19. Perkins HD, Wilson J, Raymer DP, et al. An evaluation of performance metrics for high efficiency tube-and-wing aircraft entering service in 2030-2035. NASA Technical Memorandum, http://purl.fdlp.gov/GPO/gpo20732 (2011, accessed 4 September 2017).
20. Purser P and Campbell J. Experimental verification of a simplified vee-tail theory and analysis of available data on complete models with vee tails. NACA Annual Report 1945, vol. 823, pp.237–257.
21. Heinemann P, Panagiotou P, Vratny P, et al. Advanced tube and wing aircraft for year 2050 timeframe. In: *55th AIAA aerospace sciences meeting*, Grapevine, TX, USA, 9–13 January 2017. Reston, VA: American Institute of Aeronautics and Astronautics.
22. Spalart P and Allmaras S. A one-equation turbulence model for aerodynamic flows. In: *30th aerospace sciences meeting and exhibit*, Reno, NV, USA, 1992. Reston, VA: American Institute of Aeronautics and Astronautics.
23. Spalart PR and Rumsey CL. Effective inflow conditions for turbulence models in aerodynamic calculations. *AIAA J* 2007; 45: 2544–2553.
24. Khan F. *Preliminary aerodynamic investigation of box-wing configurations using low fidelity codes*. Thesis, Lulea Univesity of Technology, Germany, 2010.

Appendix

Notation

a	airplane angle of attack
$a_{0_{Law}}$	aft wing zero-lift angle of attack
$a_{0_{Lfw}}$	forward wing zero-lift angle of attack
AR_{wing}	wing aspect ratio
b	wingspan
$C_{D_{0aw}}$	aft wing drag coefficient for zero angle of attack
$C_{D_{0fw}}$	forward wing drag coefficient for zero angle of attack
$C_{D_{0aw,wave}}$	aft wing wave drag coefficient for zero angle of attack
$C_{D_{0fw,wave}}$	forward wing wave drag coefficient for zero angle of attack
$C_{D_{0awM0.6}}$	aft wing drag coefficient for zero angle of attack at $M = 0.6$
$C_{D_{0fwM0.6}}$	forward wing drag coefficient for zero angle of attack at $M = 0.6$
C_{Dw}	wing drag coefficient
C_{Daw}	aft wing drag coefficient
C_{Dfw}	forward wing drag coefficient
C_{Dfus}	fuselage drag coefficient
C_{Dht}	horizontal tail drag coefficient
C_{Di}	induced drag coefficient
C_{DLfw}	forward wing drag coefficient due to lift
C_{Dvt}	vertical tail drag coefficient
$C_{L_{0aw}}$	aft wing lift coefficient for zero angle of attack
$C_{L_{0fw}}$	forward wing lift coefficient for zero angle of attack
$C_{L\alpha}$	airplane lift curve slope
C_{Law}	aft wing lift coefficient
C_{Lfw}	aft wing lift coefficient
$C_{L\alpha aw}$	aft wing lift curve slope
C_{Laht}	horizontal tail lift curve slope
C_{Lawf}	wing-fuselage lift curve slope
C_{L0wf}	wing-fuselage zero angle of attack lift coefficient
$d\varepsilon/da_{aw}$	downwash gradient at the aft wing
$d\varepsilon/da_{ht}$	downwash gradient at the horizontal tail
e	Oswald factor
i_{aw}	aft wing incidence angle
i_{fw}	front wing incidence angle
i_{ht}	horizontal tail incidence angle
$l_{fuselage}$	fuselage length
S_{aw}	aft wing reference surface area
S_{fw}	front wing reference surface area
S_{ht}	horizontal tail reference surface area
S_{ref}	total wing planform reference area
η_{aw}	ratio of aft wing to front wing dynamic pressure
η_{ht}	ratio of horizontal tail to front wing dynamic pressure
Γ_{aft}	dihedral aft wing
Γ_{front}	dihedral front wing
ε_h	downwash angle at the horizontal tail